Research on Engineering Structures & Materials
www.jresm.org
Research Group

Research Article

A novel high order theory for static bending of functionally graded (FG) beams subjected to various mechanical loads

Mourad Chitour[1,a], Faicel Khadraoui[1,b], Khelifa Mansouri[1,c], Billel Rebai[2,d], Abderrahmane Menasria[2,e], Amina Zemmouri[3,f], Sofiane Touati[1,g], Haithem Boumediri[*4,h]

[1]*Mechanical Engineering Department, Abbes Laghrour University, BP. 1252, Khenchela 4004, Algeria*
[2]*Civil Engineering Department, Abbes Laghrour University, BP. 1252, Khenchela 4004, Algeria*
[3]*Mechanical Engineering Department Badji Mokhtar Annaba University, Mechanics of Materials and Plant Maintenance Research Laboratory (LR3MI), Algeria*
[4]*Institut des sciences et des Techniques Appliquées (ISTA), Université Constantine 1, Algérie*

Article Info

Article history:

Received 04 Jan 2024
Accepted 31 Mar 2024

Keywords:

Functionally graded beams;
Virtual works;
Navier's method;
Deflection analysis;
Stress analysis

Abstract

This study develops a new higher-order shear deformation theory (HSDT) to analyze the static behavior of functionally graded (FG) beams under various mechanical loading conditions. The new theory is meticulously designed to effectively represent complexities in stress, strain, and deformation analysis, with a focus on maintaining or enhancing accuracy while reducing the computational burden for practical applications. The material properties of the FG beams are assumed to vary continuously across the thickness as per a power law distribution (P-FGM). The governing equilibrium equations are derived using the principle of virtual work. Navier's solution method is then utilized to obtain the analytical solutions. Extensive numerical studies are conducted to study the influences of key geometric and material parameters on the static response. The deflection, axial stress and tangential stress distributions are computed for different combinations of length-to- thickness ratio, material grading index, and applied loads. The results are validated by comparison with existing literature where good agreement is observed, demonstrating the accuracy of the proposed HSDT formulation. Parametric analyses provide useful insights into the individual and coupled effects of beam slenderness, material inhomogeneity and transverse loading on the static performance of P-FGM beams. This study enhances understanding of the structural behavior of FG beams through an efficient and accurate analytical approach.

1. Introduction

Functionally graded materials (FGMs) comprise a class of advanced composites distinguished by continuous spatial variations in composition and microstructure, resulting in corresponding property gradients across the volume [1,2]. This concept enables tailored optimization of material response and functionality by customizing the microstructural distribution. FGMs serve to mitigate challenges arising from the use of composite materials with abrupt interfaces in harsh conditions. These issues encompass stress singularities, property mismatches, inadequate adhesion, and delamination [3]. Owing to these advantages, FGMs have garnered substantial interest and adoption across diverse fields such as civil engineering, aerospace, automotive industry, general engineering applications, nuclear power plants, and more [4,5]. The graded morphology

*Corresponding author: haithem.boumediri@umc.edu.dz
[a] orcid.org/0009-0009-9087-680X; [b] orcid.org/0009-0002-3175-4377; [c] orcid.org/0000-0002-8523-6578; [d] orcid.org/0000-0003-3739-2784; [e] orcid.org/0009-0008-3507-0128; [f] orcid.org/0000-0002-6262-747X; [g] orcid.org/0000-0001-9791-0964; [h] orcid.org/0000-0002-9578-0948
DOI: http://dx.doi.org/10.17515/resm2024.141me0104rs

provides new dimensions for designing next-generation materials to meet demanding thermomechanical requirements across an array of critical applications.

Several researchers have dedicated their efforts to the mechanical analysis of Functionally Graded (FG) materials, specifically focusing on plates, beams, and shells. Their investigations have employed a range of theories and methods, encompassing both analytical and numerical approaches grounded in classical principles such as first-order shear deformation theory, higher-order shear deformation theories, and the Quasi-3D theory. In the context of FG beams, their studies have delved into the examination of free vibration and bending characteristics. Theoretical frameworks employed in these studies include well-established models such as the Euler-Bernoulli theory and the utilization of Timoshenko beam elements [6-9].

U. Kumar Kar and J. Srinivas have pioneered an elasticity solution for a rotating micro-beam subjected to thermo-mechanical loading. Their innovative approach incorporates bi-directional functional grading with graphene nanoplatelets (FG-GNPs), showcasing the potential for enhanced structural performance in challenging environments [10]. Zenkour [11] provided a precise solution for plates composed of FGM using a generalized sinusoidal shear deformation theory. Pei-Liang B et al. [12] employed a new FEM framework to analyze the mechanical responses of nanobeams made of axially functionally-graded material (FGM) under different boundary conditions. Chitour et al. [13] introduced a novel hyperbolic quasi-3D shear deformation plate theory for analyzing the bending behavior of functionally graded sandwich plate structures submitted to sinusoidal loads, while Chikh et al. [14] investigated the static response and free vibration of a functionally graded beam on elastic foundations. Thai et al. [15] explored the free vibration and bending of FG beams using higher-order beam theories, and a refined plate theory was developed for examining thermoelastic effects and wave propagation in functionally graded plates.

Ongoing research extends to dynamic analysis [16,17], stability behavior [18,19], and formulation of theories considering additional effects like porosity [20]. Investigations into beams with variable thickness and nonuniform geometries have also been undertaken [21-22]. Simultaneously, the sustained research focus on FGM beams in the mechanics, materials, and structures communities highlights their potential for tailored gradation patterns and advanced responses. This ongoing interest underscores the pivotal role FGMs play in advancing material science and structural design methodologies across various engineering applications [23-27].

This study unfolds through two integral components: a comprehensive comparative analysis and an in-depth parametric investigation. The primary objective of the comparative study is to elucidate and validate the precision and efficiency of the employed high-order shear deformation theory by systematically contrasting it with existing theories. In contrast, the parametric study systematically dissects the mechanical behavior of functionally graded beams under a spectrum of mechanical loads. It meticulously considers various factors, such as the material index (k) linked to the power-law distribution of Young's modulus, the thickness ratio (L/h) of the beams, and the specific beam type. This approach empowers the comparative evaluation, ensuring the theoretical formulation's accuracy is substantiated against alternative methodologies. Additionally, the parametric studies methodically delve into examining the influences of parameters, including the power-law distribution index, thickness ratio, beam configuration, and loading conditions, on the mechanical response of FGM beams. The study explores the coupled effects of material gradation, geometry, and external stimuli on static and dynamic performance metrics, providing a nuanced understanding of the interplay between these influential factors. This multi-faceted approach enhances the study's comprehensiveness and contributes to advancing the understanding of functionally graded beams' intricate

mechanical behavior. The integration of a comparative framework and a thorough parametric exploration not only substantiates the theory's precision but also provides valuable insights into the nuanced factors influencing the mechanical response of functionally graded beams

2. Geometry of A Functionally Graded Beams

An FG beam possesses a length (L) and a rectangular cross-section denoted by b × h, where (b) represents the width and (h) corresponds to the height [15]. The coordinates x, y, and z correspond to the length, width, and height of the beam, respectively, as depicted in Figure 1.

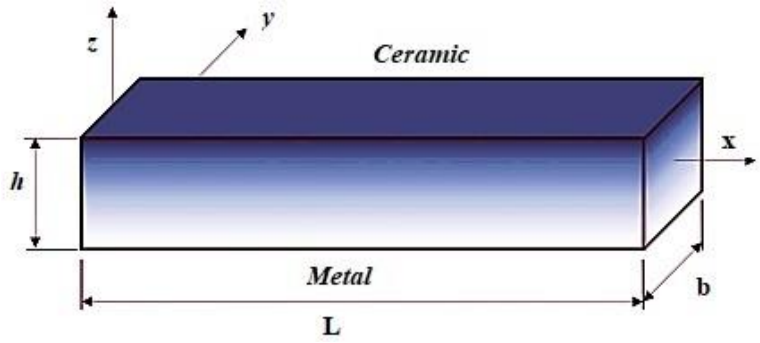

Fig. 1. Geometry and coordinate system of FG beam

The effective material properties of FGM beams, including Young's modulus (E) and mass density (ρ) that undergo smooth variations solely in the z direction. are expressed by [28]:

$$P(z) = P_m + (P_c - P_m)V_c \qquad -\frac{h}{2} \le z \le \frac{h}{2} \tag{1}$$

$$V(z) = (\frac{z}{h} + \frac{1}{2})^k, \quad V_c + V_m = 1 \tag{2}$$

The FGMs' volume fraction is assumed to conform to a power-law function along the thickness direction.

3. Displacement Field and Constitutive Equations

In this study, the emphasis is on investigating the displacement model of FG beams. A high-order shear strain theory, commonly known as the refined theory, is utilized to represent the model. The representation of the displacement model is encapsulated in the following equation:

$$\begin{aligned} u(x,z) &= u_0(x) - z\frac{\partial w_0(x)}{\partial x} + KAf(z)\frac{\partial \theta(x)}{\partial x} \\ w(x,z) &= w_0(x) \end{aligned} \tag{3}$$

uo, w and θ Are the three unknown displacement of the mid-plane of the FG beams. The specific form of the shape function f(z) is assumed by Himeur et al [29]:

$$f(z) = \sin\left(\left(\frac{z}{h}\right) - \left(\frac{4z^3}{3h^2}\right)\right) \tag{4}$$

The kinematic relations corresponding to the displacement field described in Equation (3), relying on the principles of small-strain elasticity theory, are expressed as follows:

$$\begin{aligned} \varepsilon_{xx} &= \frac{\partial u_0(x)}{\partial x} - z\frac{\partial^2 w_0(x)}{\partial x^2} + KA\, f(z)\frac{\partial \theta^2(x)}{\partial x^2} \\ \gamma_{xz} &= KA\, g(z)\frac{\partial \theta(x)}{\partial x} \end{aligned} \tag{5}$$

Where:

$$g(z) = \left(\frac{\partial f(z)}{\partial z}\right) \tag{6}$$

Based on 2D displacement field expressed in Eq. (5), the linear constitutive relations of FGM beams are assumed as:

$$\begin{Bmatrix} \sigma_{xx} \\ \tau_{xz} \end{Bmatrix} = \begin{bmatrix} C_{11} & 0 \\ 0 & C_{55} \end{bmatrix} \begin{Bmatrix} \varepsilon_{xx} \\ \gamma_{xz} \end{Bmatrix} \tag{7}$$

Where:

$$\begin{aligned} C_{11} &== E(z) \\ C_{55} &= E(z) / 2(1+\nu) \end{aligned} \tag{8}$$

4. Displacement Field and Constitutive Equations

The principal equations of equilibrium are employing the concept of virtual displacements as follows Merdaci et al [30]:

$$\delta V_{tot} = \int_V \left[\sigma_{xx}\delta\varepsilon_{xx} + \tau_{xz}\delta\gamma_{xz}\right] dV - \int_{\Omega} q\delta w(x) d\Omega = 0 \tag{9}$$

Through the integration of Equations (5) and (7) into Equation (9) across the thickness of the beams, a rephrased representation of Equation (9) is as follows:

$$\int \left[N_{xx}\frac{\partial u_0}{\partial x} - M_{xx}\frac{\partial^2 w_0}{\partial x^2} + KA\, S_{xx}\frac{\partial^2 \theta}{\partial x^2} + KA\, Q_{xz}\frac{\partial \theta}{\partial x} \right] dx - \int \left[q\delta w_0 \right] dx \tag{10}$$

Where *q* is the distributed transverse load. The stress resultants *Nxx, Mxx, Sxx and Qxz* are defined by:

$$N_{xx} = \int \sigma_{xx} dz$$
$$M_{xx} = \int \sigma_{xx} z dz$$
$$S_{xx} = \int \sigma_{xx} f(z) dz \qquad (11)$$
$$Q_{xz} = \int \tau_{xx} f'(z) dz$$

By substituting Equation (5) and Equation (7) into Equation (11), the stress and moment resultants Nxx, Mxx, Sxx and Qxz are defined as follows

$$\begin{aligned} N_{xx} &= A_{11} \frac{\partial u_0}{\partial x} - B_{11} \frac{\partial^2 w_0}{\partial x^2} + KAC_{11}^S \frac{\partial^2 q}{\partial x^2} \\ M_{xx} &= B_{11} \frac{\partial u_0}{\partial x} - D_{11} \frac{\partial^2 w_0}{\partial x^2} + KAF_{11} \frac{\partial^2 q}{\partial x^2} \\ S_{xx} &= C_{11}^S \frac{\partial u_0}{\partial x} - F_{11} \frac{\partial^2 w_0}{\partial x^2} + KAH_{11} \frac{\partial^2 q}{\partial x^2} \\ Q_{xz} &= KAG_{55} \frac{\partial q}{\partial x} \end{aligned} \qquad (12)$$

Where the stiffness components are given as follows

$$\left\{A_{11}, B_{11}, C_{11}^S, D_{11}, F_{11}, H_{11}\right\} = \int C_{11} \left\{1, z, f(z), z^2, z f(z), f^2(z)\right\} dz, \qquad G_{55} = \int C_{55} g^2(z) dz \qquad (13)$$

By performing integration by parts on Equation (10) and setting ($\delta u0$, $\delta w0$, $\delta\theta$) equal to zero, the principal differential equations from Equation (14) are obtained:

$$\begin{aligned} \delta u_0 &: \frac{\partial N_{xx}}{\partial x} = 0 \\ \delta w_0 &: \frac{\partial^2 M_{xx}}{\partial x^2} + q = 0 \\ \delta\theta &: \frac{-(KA)\partial^2 P_{xx}}{\partial x^2} + \frac{(KA)\,\partial Q_{xz}}{\partial x} = 0 \end{aligned} \qquad (14)$$

By inserting Equation (12) and Equation (13) into Equation (14), the principal equations are expressed as follows:

$$\begin{aligned} & A_{11} \frac{\partial^2 u_0}{\partial x^2} - B_{11} \frac{\partial^3 w_0}{\partial x^3} + KAC_{11}^S \frac{\partial^3 \theta}{\partial x^3} \\ & B_{11} \frac{\partial^3 u_0}{\partial x^3} - D_{11} \frac{\partial^4 w_0}{\partial x^4} + KAF_{11} \frac{\partial^4 \theta}{\partial x^4} + q = 0 \\ & -C_{11}^S \frac{\partial^3 u_0}{\partial x^3} + F_{11} \frac{\partial^4 w_0}{\partial x^4} - KAH_{11} \frac{\partial^4 \theta}{\partial x^4} + KAG_{55} \frac{\partial^2 \theta}{\partial x^2} = 0 \end{aligned} \qquad (15)$$

5. Analytical Solution

Beams are typically categorized based on the type of support they receive. In the case of simply supported FG beams, the analytical solution to the partial differential equation is achieved using the Navier method, which relies on the double Fourier series. The variables *u0, v0 and θ*, can be expressed by assuming the following variations.

$$\begin{Bmatrix} u_0 \\ v_0 \\ \theta \end{Bmatrix} = \sum_{n=1}^{\infty} \begin{Bmatrix} U_m \cos(\lambda x) \\ W_m \sin(\lambda x) \\ X_m \sin(\lambda x) \end{Bmatrix} \tag{16}$$

Where λ=mπ/a; *Um, Wm and Xm* represent arbitrary parameters to be determined. Also, the transverse load *q* is expanded in a Fourier series as:

$$q_m = \frac{2}{a}\int_0^a q(x)\sin(\lambda x)\,dx \tag{17}$$

The values of *qm* using Equation (17) are set as follows:

- Sinusoidally distributed load

$$q_m = q_0, \qquad m = 1 \tag{18}$$

- Uniform distributed load

$$q_m = \frac{4q_0}{m\pi} \tag{19}$$

- Central patch load

$$q_m = \frac{4\,q_0}{m\pi}\sin\left(m\pi\,0.02\left(l/2\right)\right) \tag{20}$$

- Central concentrated load

$$q_m = \frac{4\,Q_0}{a}\sin\left(m\pi/2\right); \quad Q_0 = q_0\,l \tag{21}$$

By substituting Equation (16) and Equation (17) into Equation (22), the resulting equations are as follows:

$$\left[L\right] = \begin{bmatrix} L_{11} & L_{12} & L_{13} \\ L_{12} & L_{22} & L_{23} \\ L_{13} & L_{23} & L_{33} \end{bmatrix} \begin{Bmatrix} U_m \\ W_m \\ X_m \end{Bmatrix} = \begin{Bmatrix} 0 \\ q_m \\ 0 \end{Bmatrix} \tag{22}$$

The elements Lij are expressed as follows:

$$
\begin{aligned}
L_{11} &= -4A_{11}\lambda^2 \\
L_{12} &= -8B_{11}\lambda^3 \\
L_{13} &= -8K_1A\,C^s_{11}\lambda^3 \\
L_{22} &= -8D_{11}\lambda^4 \\
L_{23} &= 8K_1AF_{11}\lambda^4 \\
L_{33} &= -8H_{11}K_1A\lambda^4 - 2G_{55}K_1A\lambda^2
\end{aligned}
\tag{23}
$$

6. Numerical Results and Discussion

The analysis focuses on the bending behavior response of simply-supported FG beams under various loading conditions, encompassing sinusoidal distributed, uniform, central patch, and concentrated loads. Multiple parametric studies are undertaken, and the obtained solutions are juxtaposed with available data from existing literature. The present FGM beams investigated in this study consist of a composite blend comprising Alumina (Al2O3) as the ceramic phase and Aluminum (Al) as the metal phase. The mechanical properties, including Young's modulus and Poisson's ratio, are specified in Table 1. To facilitate the analysis, the vertical displacement and stresses of the beams under various distributed loads (q) are expressed in non-dimensional terms. This allows for a more convenient comparison and understanding of the results.

Table 1. Material properties used in the FG Beams [31]

Properties	Alumina (Al2O3)	Aluminum (Al)
Young's modulus E (GPa)	380	70
Poisson's ratio ν	0.3	0.3

6.1 Validation of The Results

Tables 2, 3, and 4 provide the non-dimensional numerical results for the deflection, axial, and tangential stress of the Functionally Graded Material (FGM) beams under uniform and sinusoidal loads. These results are presented for various values of the power law index (k). The model excels in comparison to other shear deformation theories, specifically for thick beams and those with a higher power law index, due to its inclusion of thickness stretching effects. The findings indicate that a higher power law index results in a greater stiffness for FGM beams, resulting in reduced deflection and stress under uniform load. This understanding is vital for customizing FGM beams for specific purposes, as a higher power law index offers advantages such as increased stiffness and the ability to withstand higher axial loads.

Table 2. The maximum non-dimensional central deflection of FG SS beams (under uniform distribution load)

L/h	Method	*K*					
		0	**0.5**	**1**	**2**	**5**	**10**
5	Chikh Abdelbaki [32]	3.1654	4.8285	6.2594	8.0675	9.8271	10.9375
	Li et al. [33]	3.1657	4.8292	6.2599	8.0602	9.7802	10.8979
	Present	3.1653	4.8285	6.2594	8.0682	9.8317	10.9400
20	Chikh Abdelbaki [32]	2.8962	4.4644	5.8049	7.4420	8.8181	9.6905
	Li et al. [33]	2.8962	4.4645	5.8049	7.4415	8.8151	9.6879
	Present	2.8963	4.4642	5.8052	7.4419	8.8181	9.6906

Table 3. The maximum non-dimensional axial stresses of FG SS beams (subjected to an evenly distributed load)

L/h	Method	K					
		0	**0.5**	**1**	**2**	**5**	**10**
5	Chikh Abdelbaki [32]	3.8017	4.9920	5.8831	6.8819	8.1095	9.7111
	Li et al. [33]	3.8020	4.9925	5.8837	6.8812	8.1030	9.7063
	Present	3.8035	4.9943	5.8877	6.8853	8.1146	9.7158
20	Chikh Abdelbaki [32]	15.0129	19.7003	23.2052	27.0989	31.8127	38.1383
	Li et al. [33]	15.0130	19.7005	23.2054	27.0989	31.8112	38.1372
	Present	15.0133	19.7008	23.2059	27.1001	31.8136	38.1398

Table 4. The maximum non-dimensional tangential stresses of FG SS beams (Subjected to a load uniformly distributed)

L/h	Method	K					
		0	**0.5**	**1**	**2**	**5**	**10**
5	Chikh Abdelbaki [32]	0.7312	0.7484	0.7312	0.6685	0.5883	0.6445
	Li et al. [33]	0.7500	0.7676	0.7500	0.6787	0.5790	0.6436
	Present	0.7422	0.7592	0.7428	0.6802	0.6008	0.6570
20	Chikh Abdelbaki [32]	0.7429	0.7599	0.7429	0.6802	0.5998	0.6572
	Li et al. [33]	0.7500	0.7676	0.7500	0.6787	0.5790	0.6436
	Present	0.7565	0.7695	0.7540	0.6930	0.6130	0.6130

Tables 5, 6, and 7 meticulously detail the outcomes for functionally graded (FG) beams subjected to sinusoidal loads, unraveling the nuanced effects of varying power law index values. The presentation extends beyond mere reporting, incorporating a comprehensive systematic comparison with results from established beam theories, such as Chikh Abdelbaki [32], Li et al. [33], L. Hadji et al. [34], Sayyad et al. [35], and Reddy [36]. This exhaustive evaluation underscores the precision and reliability of the proposed high-order shear deformation theory in predicting the static bending behavior of FG beams under sinusoidal loads.

A granular analysis of the outcomes unveils insightful trends, particularly in the realm of deflection. Notably, there is a discernible increase in deflection with a rising volume fraction index, as evidenced in both Table 2 and Table 5. This insight underscores the pronounced influence of the power law index on the bending behavior of FG beams. The correlation is further elucidated—a higher power law index corresponds to a higher concentration of metal in the beam, resulting in a decrease in the beam's stiffness. Consequently, the beam deflects more under the same load. Similarly, the in-plane normal stress (σxx) consistently decreases with a diminishing volume fraction index (k), as observed in Table 3 and Table 6. This observation sheds light on the intricate relationship between the power law index and the distribution of normal stress within FG beams. The linkage becomes clearer—a lower power law index corresponds to a higher concentration of ceramic in the beam, which, having a lower modulus of elasticity than metal, leads to less stress under the same load.

$$\bar{w} = 100\frac{E_m h^3}{q_0 l^4} w\left(\frac{l}{2}\right), \bar{\sigma}_{xx} = \frac{h}{q_0 l}\sigma_{xx}\left(\frac{l}{2}, \frac{h}{2}\right), , \bar{\tau}_{xz} = \frac{h}{q_0 l}\tau_{xz}(0,0). \qquad (24)$$

The examination of non-dimensional tangential stresses in Table 4 and Table 7 further enriches the understanding, revealing a decrement in these stresses as the volume fraction index (k) increases. These findings collectively contribute to a nuanced comprehension of the power law index's impact on various stress components within FG beams under

sinusoidal loads. The mechanistic connection emerges—a higher power law index translates to a higher concentration of metal in the beam, resulting in a higher shear modulus than ceramic and, consequently, less shear stress under the same load.

Table 5. The maximum non-dimensional central deflection of FG SS beams under a sinusoidal load

L/h	Method	*K*			
		0	**1**	**5**	**10**
5	Hadji et al. [34]	2.5019	4.9458	7.7715	8.6526
	Sayyad et al. [35]	2.5019	4.9441	7.7739	8.6539
	Reddy [36]	2.5020	4.9458	7.7723	8.6530
	Present	2.5019	4.9458	7.7752	8.6544
20	Hadji et al. [34]	2.2839	4.5774	6.9539	7.6421
	Sayyad et al. [35]	2.2839	4.5774	6.9541	7.6422
	Reddy [36]	2.2838	4.5773	6.9540	7.6421
	Present	2.2839	4.5776	6.9538	7.6425

Table 6. The maximum non-dimensional axial stresses of FG SS beams under a sinusoidal load.

L/h	Method	*K*			
		0	**1**	**5**	**10**
5	Hadji et al. [34]	3.0913	4.7851	6.6047	7.9069
	Sayyad et al. [35]	3.0922	4.7867	6.6079	7.9102
	Reddy [36]	3.0916	4.7857	6.6057	7.9080
	Present	3.0927	4.7877	6.6092	7.9118
20	Hadji et al. [34]	12.171	18.814	25.794	30.923
	Sayyad et al. [35]	12.171	18.814	25.795	30.923
	Reddy [36]	12.171	18.813	25.794	30.999
	Present	12.171	18.815	25.796	30.923

Table 7. The maximum non-dimensional tangential stresses of FG SS beams under a sinusoidal load.

L/h	Method	*K*			
		0	**1**	**5**	**10**
5	Hadji et al. [34]	0.4755	0.4755	0.3840	0.4208
	Sayyad et al. [35]	0.4800	0.5248	0.5274	0.4237
	Reddy [36]	0.4769	0.5243	0.5314	0.4226
	Present	0.4836	0.4836	0.3928	0.4294
20	Hadji et al. [34]	0.4760	0.4760	0.3847	0.4215
	Sayyad et al. [35]	0.4806	0.5245	0.5313	0.4263
	Reddy [36]	0.4774	0.5249	0.5323	0.4233
	Present	0.4842	0.4842	0.3934	0.4302

The difference in deflection between the present method and other methods Chikh Abdelbaki [32] and Li et al. [33] as a function of the power law index k is illustrated in Figures 2 (a, b). The deviation between the deflections of FGM beams estimated by the present method and other methods depends on the power law index (k).

The difference between methods for the estimated deflection values reaches a maximum of (0.0515 for L/h = 5 and 0.003 for L/h = 20) for k = 5. Between the present method and Li et al [32] method, the difference reaches up to 0.0046 for L/h = 5 and 0.0 for L/h = 20. Between the present method and Chikh Abdelbaki [32] method, the difference is 0.008 for L/h = 5 and 0.0004 for L/h = 20, both for a value of k < 2. The difference is insignificant between methods, with the gap not exceeding 0.008 for l/h = 5 and 0.0004 for L/h = 20.

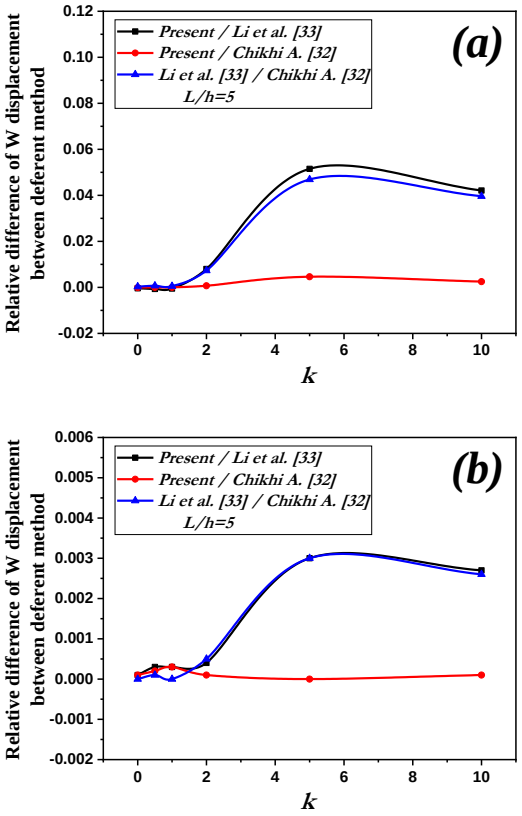

Fig. 2. Difference of non-dimensional center deflections w between different methods as a function of the power-law index k of FG S-S beams under uniform load: (a) L/h=5, (b) L/h=20

FG beams with side-to-thickness ratio L/h=5,20 is chosen in Figures 3 (a, b) and 4 (a, b). It can be seen that the deviation on the axial and tangential stress between the present model and previous one Chikh Abdelbaki [32] and Li et al. [33] is bigger for k>2 than that on for k<2. Moreover, it is also observed that the deviation on the axial and tangential stress between the present model and previous is effectively significant for thick FG s beams. The comparative analysis indicates a close correspondence between the results obtained from the proposed beam theory and the actual solutions, notably aligning well with the works of Chikh Abdelbaki [32] and Li et al. [33]. Consequently, the new beams theory can be applied to analyze the bending of FG beams.

In Figures 5, 6, 7, and 8, the effect of various types of mechanical loads (sinusoidal distributed, uniform, central patch, and concentrated load) on non-dimensional center deflections and axial stress and transversal stress is depicted, for simply supported FG beams. Figure 5 gives the changing rules of the central deflection with the power law index k. Central deflection increases monotonically with the rising value of power law index k. Meanwhile, these curves would tend to be a steady value in a value of k=5. It means that, the increasing of power law index k (beam rich in metal) would reduce the mechanical resistance of structures, rather than increasing the central deflection.

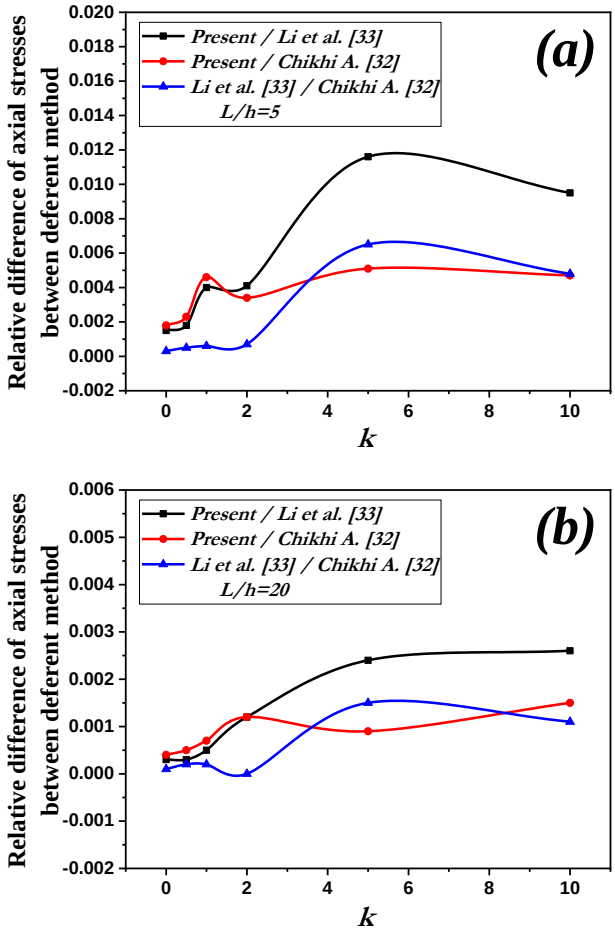

Fig. 3. Difference of non-dimensional axial stress between different methods as a function of the power-law index k of FG S-S beams subjected to an evenly distributed load: (a) L/h=5, (b) L/h=20

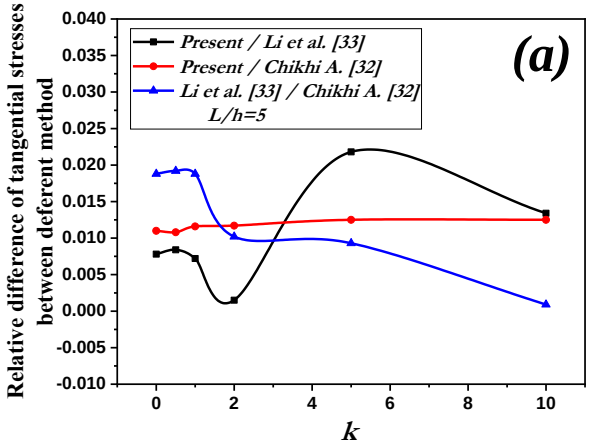

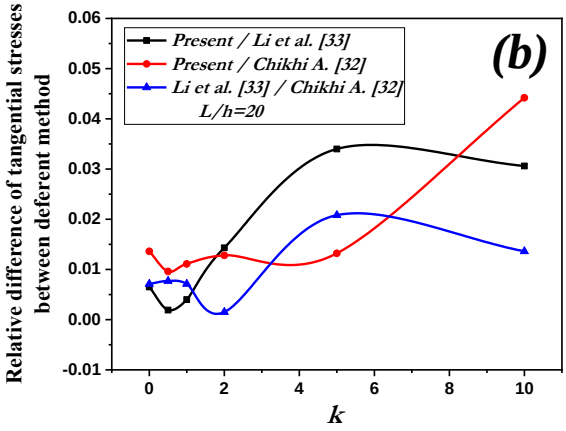

Fig. 4. Difference of tangential stress between different methods as a function of the power-law index k of FG S-S beams subjected to a load uniformly distributed: (a) L/h=5, (b) L/h=20)

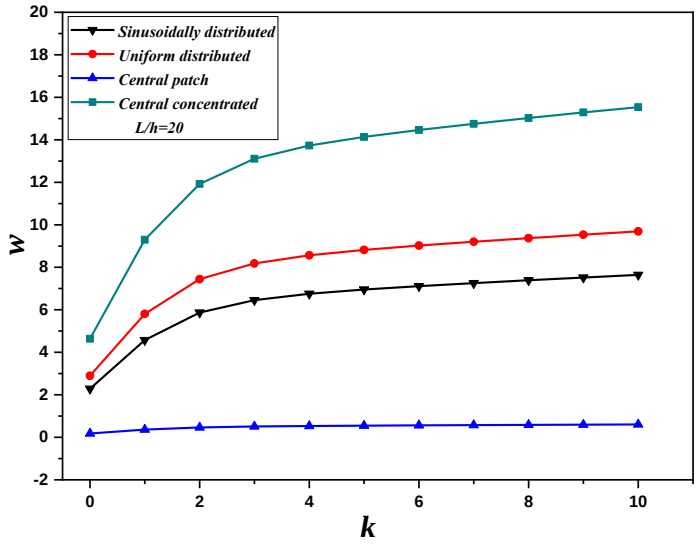

Fig. 5. Variation of the non-dimensional central deflection w versus the power-law index k of FG beams (L/h=20) exposed to diverse mechanical loading types

Figures 7 show the effect of various types of mechanical loads on distribution of normal stresses across the thickness of the FGM beam. The volume fraction exponent considered is equal to k= 1 for these results. From Figure 7 the normal stresses show that the beam works in compression up to z/h = 0.17 cases of L/h =5 and 0.14 cases of L/h=20. Then, beyond this value, the beam works only in tension. The maximum values of these stresses (longitudinal stresses), occur on the upper and lower surfaces of the plate.

In Figure 8, the non-dimensional transverse shear stresses τxz are plotted for various types of mechanical loads. the maximum transverse shear stress is directly dependent on the type of loads. Additionally, the shear stress values are relatively higher in the case of concentrated load.

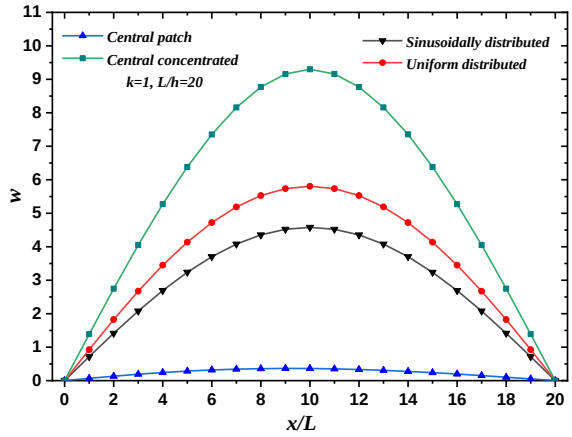

Fig. 6. Variation of the non-dimensional deflection along the length direction (L/h =20, k=1) of FG beams subjected to various types of mechanical load

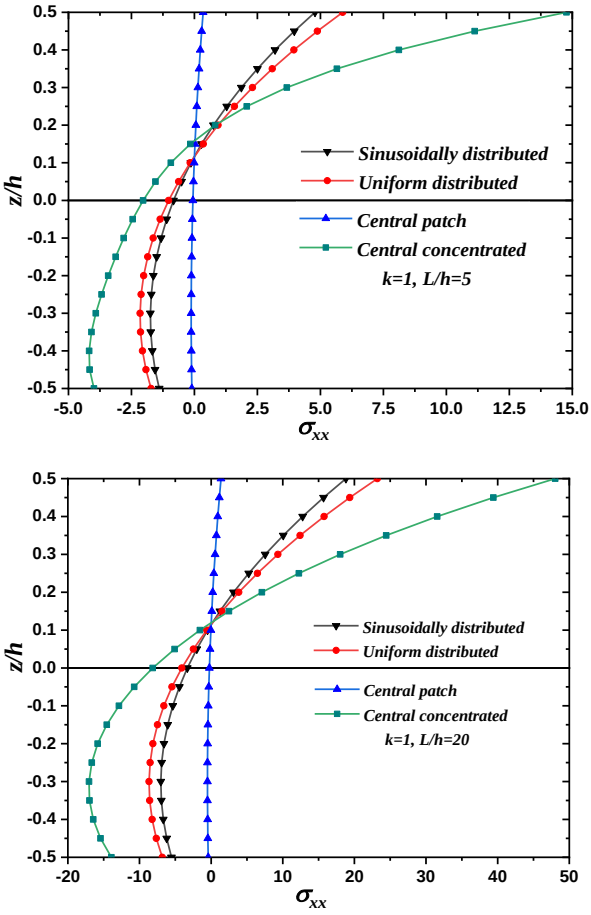

Fig. 7. Effect of various types of mechanical loads on distribution of normal stresses across the thickness of the FG beam

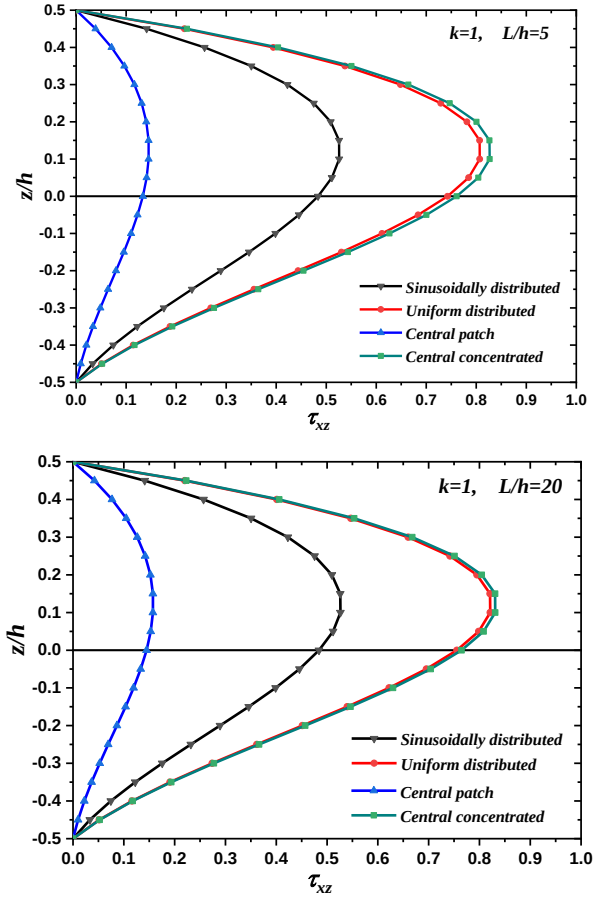

Fig. 8. effect of various types of mechanical loads on distribution of transverse shear stress across the thickness of the FG beam

7. Conclusions

This paper introduces a groundbreaking high-order shear deformation theory tailored for the static bending analysis of functionally graded (FG) beams under diverse mechanical loads. The formulation of this novel theory is meticulous, aiming to precisely capture the intricate stress, strain, and deformation behaviors inherent in FG beams, all while maintaining computational efficiency for practical applications. The governing equations, derived through the principle of virtual work, are solved analytically using Navier's method, providing a robust analytical solution that enhances our understanding of FG beam behavior.

The proposed theory undergoes extensive numerical validation, comparing favorably with existing analytical solutions and higher-order shear deformation theories. This substantiates the theory's superiority in terms of accuracy and efficiency in predicting static responses. Parametric studies investigate the individual and coupled effects of beam slenderness, material grading index, and applied load type on deflection, axial stress, and transverse shear stress distributions. The outcomes illuminate the significance of considering the thickness stretching effect, particularly for thicker beams and those with

higher power law indices, providing valuable insights into the nuanced structural behavior of FG beams.

A pivotal finding in this study reveals that an augmentation in the power-law index (k) correlates with a reduction in mechanical resistance, attributed to an increased volume fraction of metal (Vm), without a proportionate rise in central deflection. This nuanced relationship between material composition and mechanical behavior underscores the intricate nature of FG beams. The proposed theory surpasses Higher-Order Shear Deformation Theory (HSDT) in accuracy and efficiency, especially in scenarios involving thick beams and higher power law indices where the thickness stretching effect is more pronounced.

The numerical examples presented confirm the theory's accuracy in predicting deflections and stresses in FG beams subjected to uniformly distributed loads. Additionally, load type influences are explored, highlighting higher deflection and shear stress values under concentrated loads. In conclusion, the analytical solutions provided by the proposed high-order theory constitute a robust framework for comprehensively analyzing the static bending of FG beams under various mechanical loads. The theory's reliability, accuracy, and computational efficiency position it as an invaluable tool for advancing research in composite materials and structural mechanics.

References

[1] Akbaş, Ş D. Free vibration and bending of functionally graded beams resting on elastic foundation. Research on Engineering Structures and Materials, 2015; 1: 25-37. https://doi.org/10.17515/resm2015.03st0107

[2] Birman V, Byrd LW. Modeling and analysis of functionally graded materials and structures, Applied Mechanics Reviews, 2007; 60: 195-216. https://doi.org/10.1115/1.2777164

[3] Mahamood RM, Akinlabi ET. Additive manufacturing of functionally graded materials. Functionally graded materials, 2017; 47-68. https://doi.org/10.1007/978-3-319-53756-6_4

[4] Anandakumar G, Kim JH. On the modal behavior of a three-dimensional functionally graded cantilever beam: Poisson's ratio and material sampling effects. Compos. Struct, 2010; 92: 1358-1371. https://doi.org/10.1016/j.compstruct.2009.11.020

[5] Sahu RK, Sondhi L, Bhowmick S, Madan R. Deformation and stress analysis of rotating functionally graded hollow cylindrical body for variable heat generation. Res. Eng. Struct. Mater; 2023, 9: 597-616. https://doi.org/10.17515/resm2022.470me0713

[6] Alshorbagy AE, Eltaher MA, Mahmoud FF. Free vibration characteristics of a functionally graded beam by finite element method. App Math Model, 2011; 35: 412-25. https://doi.org/10.1016/j.apm.2010.07.006

[7] Eltaher MA, Emam SA, Mahmoud FF. Free vibration analysis of functionally graded size-dependent nanobeams. Appl Math Comput, 2012; 218: 7406-20. https://doi.org/10.1016/j.amc.2011.12.090

[8] Falsonea G, La Valle G. Dynamic and buckling of functionally graded beams based on a homogenization theory. Res. Eng. Struct. Mater., 2021; 7: 523-538. https://doi.org/10.17515/resm2021.259st0216

[9] Filippi M., Carrera E., Zenkour A. M. Static analyses of FGM beams by various theories and finite elements. Compos Part B-Eng. 2015; 72 1-9. https://doi.org/10.1016/j.compositesb.2014.12.004

[10] Uttam Kumar K., Srinivas. J. Vibration analysis of Bi-directional FG-GNPs reinforced rotating micro-beam under Thermo-mechanical loading. Materials Today, Proceedings, 2023; 78: 752-759. https://doi.org/10.1016/j.matpr.2022.10.227

[11] Zenkour AM. Generalised shear deformation theory for bending analysis of functionally graded plates, Appl. Math. Model., 2006; 30: 67-84. https://doi.org/10.1016/j.apm.2005.03.009
[12] Pei-Liang B, Hai Q, Tiantang Y. A new finite element method framework for axially functionally-graded nanobeam with stress-driven two-phase nonlocal integral model, Composite Structures, 2022; 295: 115769 https://doi.org/10.1016/j.compstruct.2022.115769
[13] Chitour M, Benguediab S, Bouhadra A, Bourada F, Benguediab M, Tounsi A. Effect of variable volume fraction distribution and geometrical parameters on the bending behavior of sandwich plates with FG isotropic face sheets, Mechanics Based Design of Structures and Machines, 2023; 51. https://doi.org/10.1080/15397734.2023.2197036
[14] Chikh A. Investigations in static response and free vibration of a functionally graded beam resting on elastic foundations, Frattura ed Integrità Strutturale. 2020; 51 115-126. https://doi.org/10.3221/IGF-ESIS.51.09
[15] Thai H.T, and Vo T. P. Bending and free vibration of functionally graded beams using various higher-order shear deformation beam theories. International Journal of Mechanical Sciences, 2012; 62: 57-66. https://doi.org/10.1016/j.ijmecsci.2012.05.014
[16] Khorramabadi, M.K., Jalilian, M.M. Dynamic stability analysis of functionally graded epoxy/clay nanocomposite beams subjected to periodic axial loads. J Braz. Soc. Mech. Sci. Eng., 2023; 45-61. https://doi.org/10.1007/s40430-022-03984-z
[17] Karmi Y, Tekili S, Khadri Y, Boumediri H. Vibroacoustic analysis in the thermal environment of PCLD sandwich beams with frequency and temperature dependent viscoelastic cores. Journal of Vibration Engineering & Technologies, 2023; 1-20. https://doi.org/10.1007/s42417-023-01065-6
[18] Attia A, Bousahla AA, Tounsi A, Mahmoud SR, Alwabli AS. A refined four variable plate theory for thermoelastic analysis of FGM plates resting on variable elastic foundations. Struct Eng Mech., 2018; 6 5: 453-464.
[19] Li SR, Batra RC. Relations between buckling loads of functionally graded Timoshenko and homogeneous Euler-Bernoulli beams, Composite Structures, 2013; 95: 5-9. https://doi.org/10.1016/j.compstruct.2012.07.027
[20] Benferhat R, Daouadji TH, Mansour MS. Free vibration analysis of FGM plates resting on the elastic foundation and based on the neutral surface concept using higher order shear deformation theory, Comptes Rendus Mechanique, 2016; 344: 631-641. https://doi.org/10.1016/j.crme.2016.03.002
[21] Yepeng X, Tiantang Y, Ding Z. Two-dimensional elasticity solution for bending of functionally graded beams with variable thickness, Meccanica, 2014; 49: 2479-2489. https://doi.org/10.1007/s11012-014-9958-1
[22] Rebai B. Contribution to study the effect of (Reuss, LRVE, Tamura) models on the axial and shear stress of sandwich FGM plate (Ti-6A1-4V/ZrO2) subjected on linear and nonlinear thermal loads, AIMS Materials Science, 2023;10: 26-39. https://doi.org/10.3934/matersci.2023002
[23] Esfahani SE, Kiani Y, Eslami MR. Non-linear thermal stability analysis of temperature dependent FGM beams supported on non-linear hardening elastic foundations, International Journal of Mechanical Sciences, 2013; 69: 10-20. https://doi.org/10.1016/j.ijmecsci.2013.01.007
[24] Arbind A, Reddy JN, Srinivasa AR. Modified couple stress-based third-order theory for nonlinear analysis of functionally graded beams, Latin American Journal of Solids and Structures; 2014; 11: 459-487. https://doi.org/10.1590/S1679-78252014000300006
[25] Aboudi J, Arnold SM, Pindera MJ. Response of functionally graded composites to thermal gradients, Composites Engineering, 1994; 4: 1-18. https://doi.org/10.1016/0961-9526(94)90003-5

[26] Giunta G, Crisafulli D, Belouettar S, Carrera E. A thermo-mechanical analysis of functionally graded beams via hierarchical modelling, Composite Structures, 2013; 95: 676-690. https://doi.org/10.1016/j.compstruct.2012.08.013
[27] Atteshamuddin SS., Yuwaraj MG. Bending, buckling and free vibration of laminated composite and sandwich beams: A critical review of literature, Composite Structures. 2017;171: 486-504. https://doi.org/10.1016/j.compstruct.2017.03.053
[28] Chitour M, Bouhadra A, Benguediab S, Saoudi A, Menasria AR, Tounsi A. Effect of Phase Contrast and Geometrical Parameters on Bending Behavior of Sandwich Beams with FG Isotropic Face Sheets, Journal Of Nano- And Electronic Physics, 2022: 14: 05016(6pp). https://doi.org/10.21272/jnep.14(5).05016
[29] Himeur N, Mamen B, Benguediab S, Bouhadra A, Menasria A, Bouchouicha B, Bourada F, Benguediab M, Tounsi A. Coupled effect of variable Winkler-Pasternak foundations on bending behavior of FG plates exposed to several types of loading, Steel Compost. Struct., 2022; 44: 339-355.
[30] Merdaci S, Mostefa AH, Beldjelili Y, Merazi M, Boutaleb S, Hellal H. Analytical solution for statif bending analyses of functionally grades plates with porosities. Frattura ed Integrità Strutturale. 2021; 15: 55. https://doi.org/10.3221/IGF-ESIS.55.05
[31] Menasria A, Bouhadra A, Tounsi A, Bousahl AA, Mahmoud SR. A new and simple HSDT for thermal stability analysis of FG sandwich plates. Steel and Composite Structures, 2017; 25: 157-175.
[32] Chikh A. Analysis of static behavior of a P-FGM Beam, Journal of Materials and Engineering Structures, 2019; 6: 513-524.
[33] Li XF, Wang BL, Han JC. A higher-order theory for static and dynamic analyses of functionally graded beams. Archive of Applied Mechanics. 2010; 80: 1197-1212. https://doi.org/10.1007/s00419-010-0435-6
[34] Hadji L, Bernard F, Zouatnia N. Bending and Free Vibration Analysis of Porous-Functionally Graded (PFG) Beams Resting on Elastic Foundations. Fluid Dynamic and Material Process. 2023; 19: 1043-1054. https://doi.org/10.32604/fdmp.2022.022327
[35] Sayyad AS., Ghugal YM. Analytical solutions for bending, buckling, and vibration analyses of exponential functionally graded higher order beams. Asian Journal of Civil Engineering, 2018; 19: 607-623. https://doi.org/10.1007/s42107-018-0046-z
[36] Reddy JN. A simple higher order theory for laminated composite plates. ASME Journal of Applied Mechanics, 1984; 51: 745-75 2. https://doi.org/10.1115/1.3167719